ature of 3.24 mdeg K. This is just below the lowest temperature which we have obtained. Experiments down to lower temperatures have to be done in order to separate the crystal-field–induced (local) ordering phenomenon from the cooperative ordering phenomenon.

No such quadrupole splitting is to be expected in $PrTl_3$, and the only reason for nuclear order in this compound should be the indirect coupling between nuclei outlined above. The exchange interaction constant $\mathcal{J}$ deduced from the Van Vleck susceptibility and the crystal-field splitting is less than $(0.14°K)k$, indicating that cooperative nuclear order should not occur above 0.29 mdeg K. This is not in disagreement with our observations, which indicate no nuclear ordering above 3 mdeg K. Further experiments for the detection of the cooperative ordering phenomenon are being planned.

We would like to thank C. C. Grimes and W. M. Walsh, Jr., for their constant interest and encouragement during this work.

[1]S. A. Al'tshuler, Zh. Eksperim. i Teor. Fiz.–Pis'ma Redakt. 3, 177 (1966) [JETP Letters 3, 112 (1966)].
[2]K. Andres and E. Bucher, Phys. Rev. Letters 21, 1221 (1968).
[3]K. Andres and E. Bucher, Phys. Rev. Letters 22, 600 (1969).
[4]A. C. Gossard and K. Andres, unpublished.
[5]M. A. Teplov, Zh. Eksperim. i Teor. Fiz. 53, 1510 (1967) [Soviet Phys. JETP 26, 872 (1967)].
[6]B. Bleaney, Proc. Roy. Soc. (London), Ser. A 276, 39 (1963).
[7]E. Bucher and J. P. Maita, to be published.
[8]G. T. Trammell, Phys. Rev. 131, 932 (1963).
[9]Y. L. Wang and B. R. Cooper, Phys. Rev. 172, 539 (1968).

## INELASTIC NEUTRON SCATTERING FROM $MnF_2$ IN THE CRITICAL REGION

M. P. Schulhof*† and P. Heller*†
Brandeis University, Waltham, Massachusetts 02154

and

R. Nathans
State University of New York at Stony Brook, New York 11790, and
Brookhaven National Laboratory,* Upton, New York 11973

and

A. Linz
Center for Materials Science and Engineering, Massachusetts Institute of Technology, Cambridge, Massachusetts 02139
(Received 10 April 1970)

Detailed neutron-scattering measurements have yielded the behavior of the scattering function $S(q,\omega)$ for both the transverse and longitudinal fluctuations in the critical region of the uniaxial antiferromagnet $MnF_2$. The static wavelength-dependent susceptibilities are measured both above and below $T_N$. The relaxation rates for the longitudinal fluctuations are found to be correctly described by dynamical scaling both above and below $T_N$. The scaling functions $\Omega_\pm(q/\kappa)$ applying respectively above and below $T_N$ are determined explicitly.

We have made a detailed neutron-scattering study of the static and time-dependent correlation functions in the critical region of the uniaxial antiferromagnet $MnF_2$. The static susceptibilities, both longitudinal and transverse, and the longitudinal and transverse correlation lengths have been determined for the first time in a magnetic system both above and below the critical temperature $T_N = 67.46°K$. The relaxation rates for the longitudinal and transverse fluctuations have been measured throughout the critical region. It is shown for the first time that the theory of dynamical scaling[1] provides a very good description of the longitudinal relaxation rates both above and below $T_N$. Our work follows the initial verification of dynamical scaling by Lau et al.[2] for the paramagnetic region of the isotropic antiferromagnet $RbMnF_3$. In the present work on $MnF_2$, which constitutes the most complete investigation of correlations near a second-

order magnetic phase transition yet undertaken, the scaling functions $\Omega_{\pm}(q/\kappa)$ applying respectively above and below $T_N$ are determined explicitly.

An essential part of the present work is the separation of the transverse and longitudinal fluctuations. To see how this is done, note that the cross section for the magnetic scattering of unpolarized neutrons is given by[3]

$$\frac{d^2\sigma}{d\Omega d\omega}=N\left(\frac{\gamma e^2}{mc^2}\right)\frac{K_f}{K_i}|F(\mathbf{K})|^2\left\{\sum_{\alpha\beta}(\delta_{\alpha\beta}-\hat{K}_\alpha\hat{K}_\beta)S^{\alpha\beta}(q,\omega)\right\}. \tag{1}$$

Here $\omega$ and $\vec{\mathbf{K}}=\vec{\mathbf{K}}_i-\vec{\mathbf{K}}_f$ correspond respectively to the neutron energy and momentum loss, and $\vec{q}=\vec{\mathbf{K}}-2\pi\vec{\tau}$, with $2\pi\vec{\tau}$ a magnetic reciprocal lattice vector. With $\vec{\tau}$ along [001], the curly bracketed term in (1) is such that fluctuations in each of the two transverse directions contribute to the scattering, with no contribution from the longitudinal fluctuation. With $\vec{\tau}$ along [100], however, fluctuations in the longitudinal direction and in one of the transverse directions contribute. Thus, by investigating both the [100] and [001] reflections, the transverse and longitudinal scattering functions $S_\perp(q,\omega)$ and $S_\parallel(q,\omega)$, respectively, may be separated.

We take the static cross section to be of the Ornstein-Zernike form,[3] for both the longitudinal and transverse contributions. We assume the frequency dependence of $S_\parallel(q,\omega)$ to be described by a single Lorentzian curve centered at $\omega=0$, while the frequency dependence of $S_\perp(q,\omega)$ is taken to consist of the sum of two Lorentzians displaced symmetrically about $\omega=0$ by an amount $\omega_0(q,T)$ (which may vanish). The cross sections for each of the two reflections studied then take the form

$$\left(\frac{d^2\sigma}{d\Omega d\omega}\right)_{[001]}=B(\omega,T)\frac{K_f}{K_i}\left\{\frac{A_{[001]}}{(\kappa_\perp^2+q^2)}\frac{1}{2}\left[\frac{\Gamma_\perp}{\Gamma_\perp^2+(\omega-\omega_0)^2}+\frac{\Gamma_\perp}{\Gamma_\perp^2+(\omega+\omega_0)^2}\right]\right\}, \tag{2}$$

and

$$\left(\frac{d^2\sigma}{d\Omega d\omega}\right)_{[100]}=B(\omega,T)\frac{K_f}{K_i}\left\{\frac{A_{[100]}}{(\kappa_\parallel^2+q^2)}\left[\frac{\Gamma_\parallel}{\Gamma_\parallel^2+\omega^2}\right]+\frac{\lambda A_{[100]}}{(\kappa_\perp^2+q^2)}\frac{1}{2}\left[\frac{\Gamma_\perp}{\Gamma_\perp^2+(\omega-\omega_0)^2}+\frac{\Gamma_\perp}{\Gamma_\perp^2+(\omega+\omega_0)^2}\right]\right\}, \tag{3}$$

where the factor $B(\omega,T)=\hbar\omega[1-\exp(-\hbar\omega/k_BT)]^{-1}$ expresses the requirement that the cross section for a neutron energy loss must exceed that for an equal gain by the Boltzman factor. With the exception of $\lambda$, which we assume[4] to be unity, the parameters appearing in Eqs. (2) and (3) are determined by means of a least-squares fitting procedure which folds the experimentally determined instrumental resolution function[5] with one of the cross-section expressions written above, and compares the result with the experimental data. Note that parameters $A_{[001]}$, $A_{[100]}$, $\kappa_\perp$, and $\kappa_\parallel$ depend only on the temperature $T$, while $\Gamma_\perp$, $\Gamma_\parallel$, and $\omega_0$ are to depend on both $q$ and $T$.

Data were collected for incident neutron energies of 6.6 and 13 meV, at wave vectors from $q=0$ to $q=0.258$ Å$^{-1}\simeq(0.25)2\pi\tau_{[100]}$. This was done at eleven different temperatures in a 16°K region centered on the critical temperature. The cryostat and temperature control techniques, providing 1-mdeg stability at the sample, are described elsewhere.[6] The parameters $A_{[001]}(T)$, $\kappa_\perp(q,T)$, $\Gamma_\perp(q,T)$, and $\omega_0(q,T)$ were first found from a fit to the pure transverse [001] data. Then, a fit to the [100] data permitted the determination of $A_{[100]}(T)$, $\kappa_\parallel(T)$, and $\Gamma_\parallel(q,T)$. All error limits quoted below for these quantities, or for quantities derived from them, correspond to standard deviations. Excellent fits were obtained for all of the observed data.

Using the fluctuation-dissipation theorem,[3] relative values of the static wavelength-dependent susceptibilities may now be obtained from

$$\chi_\parallel(q,T)\propto\frac{(k_BT)^{-1}A_{[100]}}{\kappa_\parallel^2+q^2} \tag{4a}$$

and

$$\chi_\perp(q,T)\propto\frac{(k_BT)^{-1}A_{[001]}}{\kappa_\perp^2+q^2}. \tag{4b}$$

In particular, relative values of the "staggered" susceptibilities are calculated from (4) by setting $q=0$. In Fig. 1 we plot the results for the longitudinal staggered susceptibility $\chi_\parallel(0,T)$ both above and below $T_N$. This figure includes data obtained in our earlier quasielastic experiment,[6] the constant of proportionality being adjusted for agreement with the present data at the highest temperature. On fitting the combined data of Fig. 1 to $\chi_\parallel(T)=b_+(T-T_N)^{-\gamma}$ for $T>T_N$ and $\chi_\parallel(T)=b_-(T_N-T)^{-\gamma'}$ for $T<T_N$, we obtain $\gamma=1.27\pm0.02$, $\gamma'=1.32\pm0.06$, and $b_+/b_-=4.8\pm0.5$.

The behavior of the longitudinal wavelength-dependent susceptibility for $q\neq0$ may be described

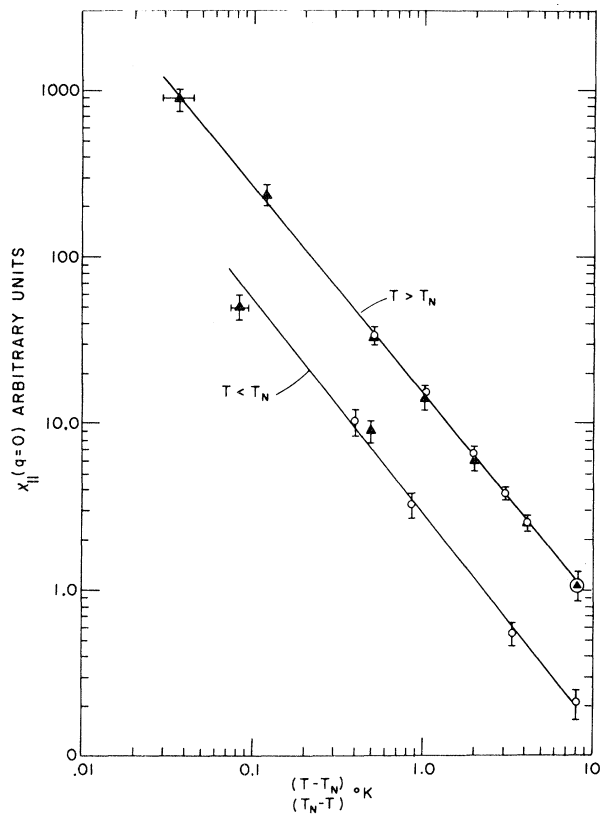


FIG. 1. Temperature dependence of the longitudinal staggered susceptibility above and below $T_N$. The open circles are obtained from the present inelastic-scattering data, the closed triangles from an earlier energy-unresolved scattering experiment (Ref. 6), normalized to the present data at 76°K.

by Eq. (4a) by specifying $\kappa_{\parallel}(T)$. On fitting our data by $\kappa_{\parallel}(T) = \kappa_{+}(T-T_N)^{\nu}$ for $T > T_N$ and $\kappa_{\parallel}(T) = \kappa_{-}(T_N-T)^{\nu'}$ for $T < T_N$ we find

$$\nu = 0.634 \pm 0.02, \quad \nu' = 0.56 \pm 0.05,$$
$$\kappa_{+} = (0.032 \pm 0.004)\ \text{Å}^{-1}\ (^{\circ}\text{K})^{-\nu},$$
$$\kappa_{-} = (0.055 \pm 0.006)\ \text{Å}^{-1}\ (^{\circ}\text{K})^{-\nu'}. \qquad (5)$$

Our data for the transverse susceptibilities, the transverse relaxation rates, and the spin-wave energy gap, will be presented in a more detailed communication.

Of paramount interest here is the behavior of the longitudinal relaxation rates $\Gamma_{\parallel}(q, t)$. Our results are shown graphically in Fig. 2. Above $T_N$, the decay rates vary rather slowly with temperature, except for $q = 0$ where we find an essentially linear temperature dependence, $T > T_N$:

$$\Gamma_{\parallel}(0, T) = (2.1 \pm 0.1\ \text{meV}) \times [(T-T_N)/T_N]^{0.95 \pm 0.05}. \qquad (6)$$

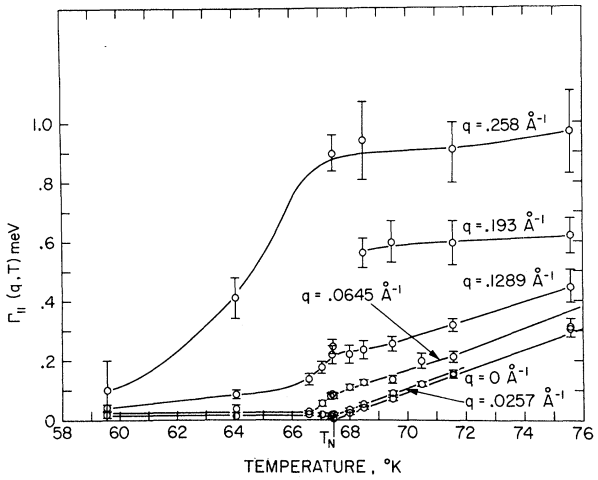


FIG. 2. Relaxation rate of the longitudinal spin fluctuations as a function of temperature and wave vector in the critical region.

The situation is completely different below $T_N$, where $\Gamma_{\parallel}$ apparently vanishes as $q \to 0$ at all temperatures. Our data are consistent with a diffusive behavior $\Gamma_{\parallel}(q, T) \cong D(T)q^2$. Actually, finite instrumental resolution prevented us from measuring $\Gamma_{\parallel}$ exactly at $q = 0$, since a magnetic Bragg peak dominates the scattering there.

For $T = T_N$, our data are well fitted by the expression

$$\Gamma_{\parallel}(q, T_N) = (7.0 \pm 0.9\ \text{meV})q^{1.6 \pm 0.2}, \qquad (7)$$

where $q$ is expressed in Å$^{-1}$. Equation (7) correctly describes our data for $0.026\ \text{Å}^{-1} < q < 0.2\ \text{Å}^{-1}$. The work of Riedel and Wegner[7] predicts a change in the power-law behavior close to the critical point due to the effects of anisotropy. On account of resolution limitations, it is simply not possible for us to say whether a different power law might apply for smaller $q$ values. Similarly, although Eq. (6) correctly describes our data for $0.5 < T-T_N < 9$°K, we simply cannot say whether a different exponent might apply for smaller $T-T_N$ just above the critical point.

Dynamical scaling predicts[1] that the exponent expressing the dependence of $\Gamma_{\parallel}(0, T)$ on $\kappa_{\parallel}(T)$ above $T_N$ should equal the exponent expressing the $q$ dependence of $\Gamma_{\parallel}$ and $T_N$. Indeed, using (6) and (5) we find, for $T > T_N$,

$$\Gamma_{\parallel}(0, T) = (6.6 \pm 0.6\ \text{meV})[\kappa_{\parallel}(T)]^{1.49 \pm 0.07}, \qquad (8)$$

where $\kappa_{\parallel}$ is expressed Å$^{-1}$. The exponents in (7) and (8) do in fact agree to within experimental error. More generally, dynamical scaling predicts that

$$\Gamma_{\parallel}(q, T) = [\kappa_{\parallel}(T)]^{z}\, \Omega_{\pm}[q/\kappa_{\parallel}(T)], \qquad (9)$$

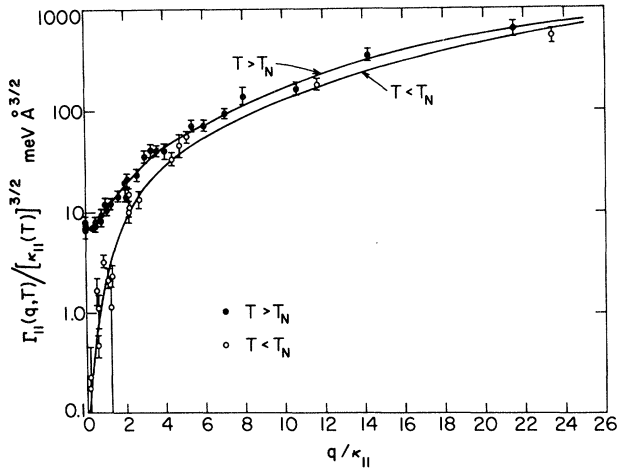


FIG. 3. A replot of the data of Fig. 2 in the form suggested by the theory of dynamical scaling. The ordinate is the scaled longitudinal relaxation rate, the abscissa the scaled wave vector. The two curves are the two branches of the longitudinal dynamical scaling function.

where the ± signs apply respectively above and below $T_N$. To test Eq. (9), we have replotted the data of Fig. 2 in Fig. 3. Here, the ordinate is $\Gamma_{\parallel}(q, T)/[\kappa_{\parallel}(T)]^z$, and the absicissa is $q/[\kappa_{\parallel}(T)]$. In making this plot, we have taken $z = \frac{3}{2}$, which is consistent with both (7) and (8). The data for $T > T_N$ and $T < T_N$ are represented respectively by the solid and open circles. Note that all of the data of Fig. 2 are present in the two curves of Fig. 3. The two curves represent the two branches of the scaling function; they merge for large $q/\kappa$, as must be the case, since this represents the behavior close to $T_N$. For each branch, the data points are intermixed over the curve: There is no systematic departure from it as a function of $T$ or $q$. This kind of plot is reminiscent of the original representations of static scaling phenomena.[8]

The two branches of the scaling function have quite different behaviors for small values of $q/\kappa$. Thus, above $T_N$ we find

$$\Omega_+(q/\kappa) = [6.9 + 2.6(q/\kappa)^2 + \cdots] \text{ meV Å}^{3/2}, \quad (10a)$$

while below $T_N$ we have

$$\Omega_-(q/\kappa) = [1.8(q/\kappa)^2 + \cdots] \text{ meV Å}^{3/2}. \quad (10b)$$

The absence of the constant term in (10b) is a reflection of the diffusive behavior observed below $T_N$. A theory for this has been advanced by one of us[9] (P.H.) and, independently, by Halperin and Hohenberg.[10] According to this view, the diffusive central peak for the longitudinal fluctuation below $T_N$ is a manifestation of thermal diffusion taking place within the spin system. The diffusion constant $D(T)$ should then equal the ratio of the spin system thermal conductivity to the magnetic specific-heat density, in analogy with the Landau-Placzek theory for fluids.

In conclusion, we have made a complete study of the static and dynamic correlations near the second-order phase transition in $MnF_2$. We find that dynamical scaling provides a remarkably successful description of our data. The scaling functions applying respectively above and below $T_N$ are found to have quite different behaviors for small values of $q/\kappa$.

We gratefully acknowledge many fruitful discussions with Dr. P. Hohenberg, Dr. M. Blume, Professor R. Ferrell, Professor P. Martin, and Professor R. B. Griffiths. Interest and advice were also generously given by Dr. G. Shirane, Dr. L. Corliss, and Dr. J. Hastings.

---

*Work performed under the auspices of the U. S. Atomic Energy Commission.

†Work supported by the Air Force Office of Scientific Research, Grant No. AF68-1480.

[1]B. I. Halperin and P. C. Hohenberg, Phys. Rev. 177, 952 (1969), and references contained therein, including references to the original work of R. Ferrell and coworkers on liquid helium.

[2]H. Y. Lau, L. M. Corliss, A. Delapalme, J. M. Hastings, R. Nathans, and A. Tucciarone, Phys. Rev. Letters 23, 1225 (1969).

[3]W. Marshall and R. Lowde, Rep. Progr. Phys. 21, 705 (1968).

[4]A theoretical discussion of $\lambda$, together with an experimental verification of the value $\lambda = 1$ will be presented in a more detailed report.

[5]M. J. Cooper and R. Nathans, Acta Cryst. 23, 357 (1967).

[6]M. P. Schulhof, P. Heller, R. Nathans, and A. Linz, Phys. Rev. B 1, 2304 (1970).

[7]E. Riedel and F. Wegner, Phys. Rev. Letters 24, 730 (1970).

[8]See, for example, A. Arrott and J. E. Noakes, Phys. Rev. Letters 19, 786 (1967); M. S. Green, M. Vicentini-Missoni, and J. M. H. Levelt-Sengers, Phys. Rev. Letters 18, 1113 (1967).

[9]P. Heller, to be published.

[10]B. I. Halperin and P. C. Hohenberg, Phys. Rev. 188, 898 (1969).